Japan J. Indust. Appl. Math., 25 (2008), 281–303 Area ⟨1⟩

Deviation from the Predicted Wavenumber in a Mode Selection Problem for the Turing Patterns

Masataka Kuwamura

Graduate School of Human Development and Environment
Kobe University, Kobe 657–8501, Japan
E-mail: kuwamura@main.h.kobe-u.ac.jp

Received March 14, 2007
Revised March 05, 2008

In this paper, we investigate a mode selection problem for the Turing patterns generated from small random initial disturbances in one-dimensional reaction-diffusion systems on a sufficiently large domain. For this problem, it is widely accepted that the maximizer of the dispersion relation give rise to the wavenumber to be selected. Even in a small neighborhood of the bifurcation point, our numerical experiments show that this is not always true.

Key words: Turing pattern, mode selection, dispersion relation

1. Introduction

In various biological phenomena, many interesting macro-scopic spatial patterns are self-organized such as formation and development of embryo, animal coat, and so on. A theoretical approach for understanding such pattern formation mechanism was initiated by a simple but profound idea of Turing [13] that chemicals can react and diffuse in such a way as to produce inhomogeneous spatial structures. This original idea has been refined through applications to bifurcation problems in reaction-diffusion systems. Roughly speaking, if one varies a parameter in a reaction-diffusion system, then a spatially uniform steady state of the system becomes unstable, and there appear other stable steady states with spatial structure. They are called the Turing patterns which exhibit spatially periodic structure near the bifurcation point.

In such a situation, we are interested in what pattern is to be uniquely selected among many bifurcating solutions. It is a typical and fundamental problem in pattern formation theory, known as pattern selection problem. As evidenced in [2, 10, 11], such problem has been intensively studied and selection criteria have been proposed since the early 1980's. These criteria have been influential and played very important roles in various pattern selection problems, however, from a mathematical viewpoint, they are not fully understood.

In this paper, we investigate a mode selection problem for the Turing patterns generated from small random initial disturbances in one-dimensional reaction-diffusion systems on a sufficiently large domain under the periodic boundary conditions. Although our problem looks quite elementary, there are very few literatures which treat such a problem from a comprehensive viewpoint. For example, [10, Section 14.6] gives a brief explanation as follows. "If the initial con-

ditions consist of small random perturbations about the uniform steady state then the likely pattern to evolve is that with the largest linear growth." In other words, the maximizer of the dispersion relation exactly corresponds to the wavenumber of the Turing pattern to be selected near the bifurcation point. This is a widely accepted criterion and seems to be consistent to our naive intuition. However, is it true that the Turing pattern to be selected is really determined by such a simple criterion? We propose a condition under which the criterion is most likely valid in many practical applications, and give examples for which such criterion fails.

Pattern selection is a subject of broad interest, not only from mathematical analysis but also from various fields of sciences such as biological morphology, chemical reaction, thermal convection, crystal growth, and so on. Therefore, we present essential points of our results in such a manner to allow those who are interested in pattern selection problems. The organization of this paper is as follows: In the next section, we review a mode selection problem for the Turing patterns and explain about the selection criterion through a concrete example. In Section 3, we examine the dynamics around the uniform steady state of the example, and propose a practical condition to guarantee the validity of the criterion. Then, near the bifurcation point, where nonlinearity is not significant, we exhibit numerical examples which indicate that the criterion fails. In Section 4, we point out some relevant subjects and further problems related to the results presented in the previous sections. In Section 5, we conclude with a summary of this paper.

2. Mode selection of the Turing patterns in one-dimensional reaction-diffusion systems

In this section, we review a mode selection problem for the Turing patterns near the bifurcation point through a simple reaction-diffusion system of activator-inhibitor type.

Let us consider

$$\begin{cases} \tau_1 u_t = d_1 u_{xx} + \alpha u - \sigma u^3 - \beta v, \\ \tau_2 v_t = d_2 v_{xx} + \beta u - \gamma v, \end{cases} \tag{2.1}$$

where $\tau_1, d_1, d_2, \alpha, \beta, \gamma, \sigma > 0$ and $\tau_2 \geq 0$. (2.1) is a reaction-diffusion system with the FithHugh–Nagumo mechanism, which has been intensively studied in many literatures ([10, 11] and the references therein). We begin to construct the Turing patterns which are bifurcating stationary solutions of (2.1). Let $(\bar{u}, \bar{v}) = (0, 0)$ be a spatially uniform steady state of (2.1), which is an onset of bifurcating patterns. We consider a situation in which $(\bar{u}, \bar{v})$ loses its stability and gives rise to the appearance of spatially periodic stationary solutions. To do so, we consider the linearized eigenvalue problem at $(\bar{u}, \bar{v}) = (0, 0)$

$$Tw_t = Dw_{xx} + Bw, \tag{2.2}$$

where $w = (w_1, w_2)^{\mathrm{T}} \in \mathbf{C}^2$ and

$$T = \begin{pmatrix} \tau_1 & 0 \\ 0 & \tau_2 \end{pmatrix}, \quad D = \begin{pmatrix} d_1 & 0 \\ 0 & d_2 \end{pmatrix}, \quad B = \begin{pmatrix} \alpha & -\beta \\ \beta & -\gamma \end{pmatrix}.$$

We are looking for solutions of the following form:

$$w = \Psi_k \exp(\lambda t + ikx), \quad \Psi_k \in \mathbf{C}^2. \tag{2.3}$$

Substituting (2.3) into (2.2), we obtain a system of linear equations

$$(\lambda T + sD - B)\,\Psi_k = 0, \tag{2.4}$$

where $s = k^2$, $\langle \Psi_k, \Psi_k \rangle = 1$. In order for a stationary solution to bifurcate from $\bar{u}$, it is necessary that (2.4) possesses a non-trivial solution for $\lambda = 0$. Hence it follows from $\det(sD - B) = 0$ that

$$\beta^2 - (\alpha - sd_1)(\gamma + sd_2) = 0, \tag{2.5}$$

so that (2.4) has nontrivial solution $\Psi_k = (p_k, q_k)^{\mathrm{T}}$ for $\lambda = 0$, where

$$p_k^2 = \frac{\beta^2}{\beta^2 + (\alpha - sd_1)^2} \quad \text{and} \quad q_k^2 = \frac{(\alpha - sd_1)^2}{\beta^2 + (\alpha - sd_1)^2}. \tag{2.6}$$

Here we choose d_2 as a Turing bifurcation parameter. By using (2.5), we have

$$d_2 = \hat{d}_2(s) = \frac{\beta^2}{s(\alpha - sd_1)} - \frac{\gamma}{s}$$

for $0 < s < \alpha/d_1$. Notice that $d_2 = \hat{d}_2(s)$ does not depend on τ_1 and τ_2. By using $\hat{d}_2' = 0$, we have

$$s_c = k_c^2 = \frac{\alpha\sqrt{\beta^2 - \alpha\gamma}}{d_1(\beta + \sqrt{\beta^2 - \alpha\gamma})} > 0 \tag{2.7}$$

and

$$d_2^c = \hat{d}_2(s_c) = \frac{d_1(\beta + \sqrt{\beta^2 - \alpha\gamma})^2}{\alpha^2}, \tag{2.8}$$

and obtain the following graph of $d_2 = \hat{d}_2(s)$ as in Fig. 1.

Furthermore, we suppose that a quadratic equation in λ

$$G(\lambda, s; d_2) := \det(\lambda T + sD - B) = 0$$

gives the dispersion relations

$$\lambda_j = \lambda_j(s; d_2) \quad (j = 1, 2) \tag{2.9}$$

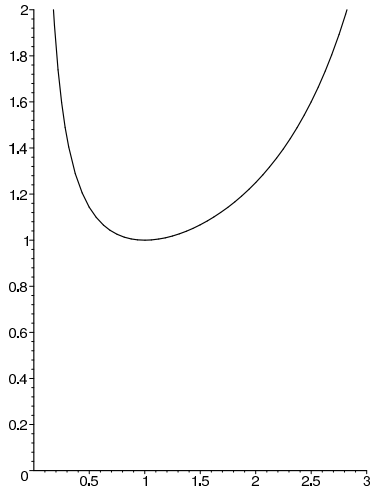

Fig. 1. The graph of $d_2 = \hat{d}_2(k^2)$ when $d_1 = 0.25$, $\alpha = 1.0$, $\beta = 1.5$, $\gamma = 2.0$. In this case, the bifurcation point is given by $(k_c, d_2^c) = (1.0, 1.0)$. The Turing patterns appear for $d_2 > \hat{d}_2(k^2)$.

satisfying the following properties:

$$\operatorname{Re}\lambda_1(s; d_2) < 0 \text{ for all } s \text{ and } d_2 < d_2^c, \tag{2.10}$$

$$\lambda_1(s_c; d_2^c) = 0 \text{ and } \operatorname{Re}\lambda_1(s; d_2^c) < 0 \text{ for } s \neq s_c, \tag{2.11}$$

$$\lambda_1(s; d_2) \text{ is real valued near the bifurcation point } (s_c, d_2^c), \tag{2.12}$$

$$\frac{\partial}{\partial d_2}\lambda_1(s; d_2)\bigg|_{(s,d_2)=(s_c,d_2^c)} > 0, \tag{2.13}$$

$$\operatorname{Re}\lambda_2(s; d_2) < 0 \text{ for all } s \text{ and } d_2. \tag{2.14}$$

Note that the dispersion relations are dependent on τ_1 and τ_2. $\lambda_1 = \lambda_1(s; d_2)$ is called the *critical dispersion relation*, which plays a central role in the subsequent analysis. It is corresponding to the maximum of the real parts of the roots of $G(\lambda, s; d_2) = 0$. Fig. 2 shows a typical example of the behavior of $\lambda_1 = \lambda_1(s; d_2)$ near $d_2 = d_2^c$. The conditions (2.10)–(2.14) guarantee that the rest state $(\bar{u}, \bar{v}) = (0, 0)$ is stable for $d_2 < d_2^c$. If $d_2 > d_2^c$, then $(\bar{u}, \bar{v}) = (0, 0)$ becomes unstable, and the instability for the direction of the Fourier mode $\exp(\pm kx)$ corresponding to $\lambda_1 = \lambda_1(s; d_2) > 0$ $(s = k^2)$ grows up, and another stable steady state appears. It should be noted that the mode with the largest growth rate is given by the maximizer of the critical dispersion relation.

In what follows, we abbreviate "the critical dispersion relation" to "the dispersion relation" unless any confusion does occur.

Under the above assumptions, we can construct the Turing patterns

$$\phi(x; k, d_2) = ae^{ikx}\,\Psi_k + \text{c.c.} + \text{h.o.t.} \tag{2.15}$$

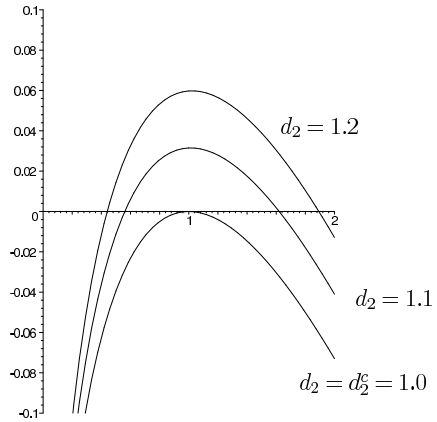

Fig. 2. The behavior of the critical dispersion relation $\lambda_1 = \lambda_1(s; d_2)$ for $d_2 = 1.0, 1.1, 1.2$ when $d_1 = 0.25$, $\alpha = 1.0$, $\beta = 1.5$, $\gamma = 2.0$, $\tau_1 = \tau_2 = 1.0$. It is corresponding to the maximum of the real parts of the roots of $G(\lambda, s; d_2) = 0$.

for $d_2 > \hat{d}_2(k^2)$ near the bifurcation point (k_c, d_2^c) provided

$$0 < \alpha < \gamma \quad \text{and} \quad \beta^2 - \alpha\gamma > 0, \tag{2.16}$$

where $\Psi_k = (p_k, q_k)^{\mathrm{T}}$ is given by (2.6), and c.c. and h.o.t. denote the complex conjugate and higher order terms with respect to a, respectively. $a = a(k, d_2 - \hat{d}_2(k^2)) \geq 0$ denotes the amplitude of the Turing patterns, which is sufficiently small with $a(k, 0) = 0$. Roughly speaking, it is determined as follows: Substituting (2.15) into

$$d_1 u_{xx} + \alpha u - \sigma u^3 - \beta v = 0 \quad \text{and} \quad d_2 v_{xx} + \beta u - \gamma v = 0, \tag{2.17}$$

and solve (2.17) with respect to a by using a standard procedure known as the Liapunov–Schmidt method. For more details, see textbooks [5, 10]. In this case, we can easily check (2.10)–(2.14) and obtain

$$\phi(x; k, d_2) = 2\sqrt{\frac{(d_2 - \hat{d}_2(k^2))k^2}{3\sigma}}\cos(kx)\begin{pmatrix} \alpha - d_1 k^2 \\ (\alpha - d_1 k^2)^2 \end{pmatrix} + \text{h.o.t.}$$

Notice that σ which characterize the intensity of nonlinearity affects on the amplitude of the Turing pattern, but not on the wavenumber explicitly.

Remark 1. The Turing patterns which we construct are obtained in a *weakly nonlinear* region near the bifurcation point, where standard local analysis such as the bifurcation theory [5] and the reductive perturbation method [6] are effective. In other words, we do not deal with situations in which the intensity of nonlinearity is strong or a bifurcation parameter is far away from the bifurcation point.

From the above argument, we see that there is a family of the Turing patterns parameterized by the wavenumber k for each fixed $d_2 > d_2^c$ near the bifurcation point. We now investigate what Turing pattern is to be uniquely selected among many near the bifurcation point. To do so, we numerically solve (2.1) with a small random initial data on a sufficiently large domain for a sufficiently large time interval, i.e.,

$$\begin{cases} \tau_1 u_t = d_1 u_{xx} + \alpha u - \sigma u^3 - \beta v, \quad \tau_2 v_t = d_2 v_{xx} + \beta u - \gamma v, \\ u(x,0) = \varepsilon u_0(x), \quad v(x,0) = \varepsilon v_0(x), \quad 0 < x < L, \quad 0 < t < T, \end{cases} \tag{2.18}$$

where $u_0(x), v_0(x) \in (-1/2, 1/2)$ are uniform distributions generated by pseudo-random numbers. Here we impose the periodic boundary condition on (2.18) because the spectral properties of the linearized eigenvalue problem at a stationary solution of (2.1) on the whole domain are well approximated to that of (2.18) with the periodic boundary conditions. We examine the final state of a solution of (2.18), i.e., the spatial profile and the Fourier power spectrum of $u(x,T)$ for sufficiently large T.

From the above argument, we may expect that $u(x,T)$ is sufficiently close to the Turing pattern $\phi(x;k,d_2)$ with the wavenumber corresponding to the maximizer of the critical dispersion relation $\lambda_1 = \lambda_1(s;d_2)$ defined by $G(\lambda, s; d_2) = 0$.

Differentiating $G(\lambda, s; d_2) = 0$ with respect to s, we obtain $G_\lambda \cdot \lambda'(s) + G_s = 0$, so that

$$\lambda'(s) = -G_s/G_\lambda. \tag{2.19}$$

We solve $G_s = 0$ under the condition $G = 0$. It follows from $G_s = 0$ that

$$\lambda = \frac{\alpha d_2 - \gamma d_1 - 2d_1 d_2}{d_2\tau_1 + d_1\tau_2}.$$

Substituting this into $G = 0$, it turns out that the maximizer of the critical dispersion relation is given by

$$s = k_u^2(d_2) := \frac{\beta(d_2\tau_1 + d_1\tau_2) - \sqrt{d_1 d_2}(\gamma\tau_1 + \alpha\tau_2)}{\sqrt{d_1 d_2}(d_2\tau_1 - d_1\tau_2)}, \tag{2.20}$$

which may determine the wavenumber of the Turing pattern to be uniquely selected. Hereafter, we denote by $k_u(d_2)$ the maximizer of the critical dispersion relation.

We now numerically solve (2.18) for $d_2 = 1.20$ by using the pseudo-spectral method and the discrete FFT when

$$\begin{aligned} &d_1 = 0.25, \quad \alpha = 1.0, \quad \beta = 1.5, \quad \gamma = 2.0, \\ &\tau_1 = \tau_2 = 1.0, \quad \sigma = 1.0 \quad \text{and} \quad \varepsilon = 0.0001. \end{aligned} \tag{2.21}$$

This method is the only one which gives reliable numerical solutions of (2.18) on a sufficiently large domain under the periodic boundary conditions in a small

neighborhood of the bifurcation point [4]. In this case, the bifurcation point is given by $(k_c, d_2^c) = (1.0, 1.0)$. We set $L = 200\pi$ so that the discrete FFT can detect a variation of the wavenumber of the Turing pattern in the accuracy $\delta k = 2\pi/L = 0.01$. Fig. 3 shows some examples of the spatial profile and the Fourier power spectrum of $u(x, T)$ for $T = 3000$, where T is determined by the time when a solution of (2.18) reaches a (meta)stable steady state.

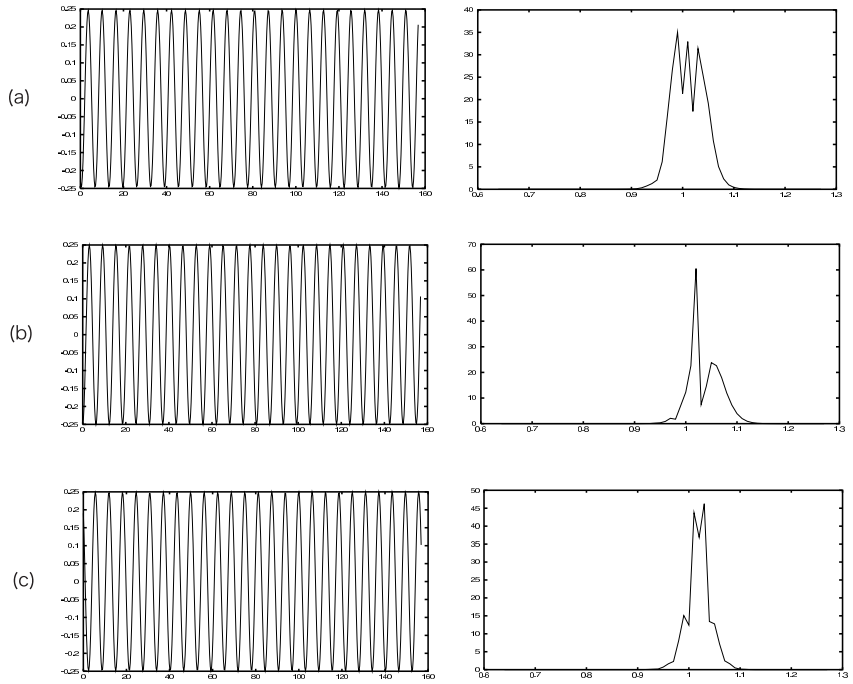

Fig. 3. Some examples of the spatial profile and the Fourier power spectrum of $u(x, T)$. They are presented in windows $0 \le x \le 50\pi$ and $0.64 \le k \le 1.28$, respectively.

As seen in Fig. 3, the Fourier power spectrum does not necessarily have a clear (bell) shape while the spatial profile looks like a sinusoidal function with a particular wavenumber. Therefore we compute the power spectra of $u(x, T)$ for 30 random initial data, and take their average. The result is as follows:

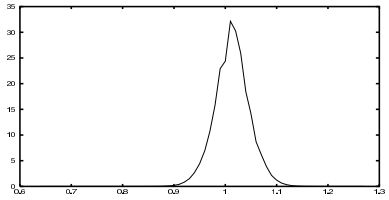

k	0.96	0.97	0.98	0.99	1.00	1.01
$\hat{u}(k)$	6.95	10.71	15.82	22.93	24.37	32.14

k	1.02	1.03	1.04	1.05	1.06	1.07
$\hat{u}(k)$	30.27	25.94	18.41	14.10	8.69	6.20

Fig. 4. The average of the Fourier power spectra of $u(x, T)$ for 30 random initial data.

The above result shows that the wavenumber $k = 1.01$ is selected with the highest probability. We call this wavenumber the *selected wavenumber* denoted by $k_s = k_s(d_2)$. In this case, $k_s(1.20) = 1.01$, which implies that $k_s(1.20) \approx k_u(1.20)$ by virtue of (2.20). Notice that $k_s(d_2)$ is a statistical quantity while $k_u(d_2)$ is a deterministic one.

Similarly, solving (2.18) numerically for $d_2 = 1.05$ and $d_2 = 1.10$ under the same parameters as above, we obtain the following results:

Table 1. The selected wavenumber $k_s(d_2)$ for $d_2 = 1.05$, 1.10 and 1.20.

d_2	1.05	1.10	1.20
$k_u(d_2)$	1.00	1.01	1.01
$k_s(d_2)$	1.00	1.01	1.01

We emphasize that the selected wavenumber $k_s(d_2)$ do not depend on σ the coefficient of the nonlinear term because the almost same numerical results as Tables 2 and 3 are obtained for $\sigma = 0.1$ and $\sigma = 10$. More precisely, σ affects on the amplitude of the Turing pattern to be selected, but not on the wavenumber explicitly. This implies that our numerical experiments are done in a small neighborhood of the bifurcation point.

In this case, considering the accuracy of our numerical computations, Table 1 shows that $k_s(d_2) \approx k_u(d_2)$, which supports that the Turing patten observed with the highest probability can be given by the maximizer of the critical dispersion relation.

Thus, we see that our mode selection problem for the Turing patterns is a *statistical* one. Moreover, the above example supports a widely accepted criterion that the wavenumber of the Turing pattern generated from a small random initial disturbance can be predicted by the maximizer of the critical dispersion relation. In the next section, we give a supporting argument for the above numerical results and exhibit numerical examples which indicate that the criterion fails.

3. Deviation from the predicted wavenumber of the Turing patten

In this section, we examine the dynamics of (2.18) around the uniform steady state, and propose a practical condition to guarantee that the wavenumber of the Turing pattern observed with the highest probability is given by the maximizer of the dispersion relation. Then we give examples for which the criterion fails.

In the previous section, we numerically solved (2.18) for $d_2 = 1.20$ by using the pseudo-spectral method and the discrete FFT under the values of parameters (2.21). The following pictures in Fig. 5 show the dynamics of solutions for (2.18) around the uniform steady state.

As seen Fig. 5, every numerical solution starting from a random initial data quickly goes to the uniform steady state $(\bar{u}, \bar{v}) = (0, 0)$, and stay in a small neighborhood of $(\bar{u}, \bar{v}) = (0, 0)$ for some time, and then evolves into the Turing pattern as time passes. This implies that near the bifurcation point, the uniform steady

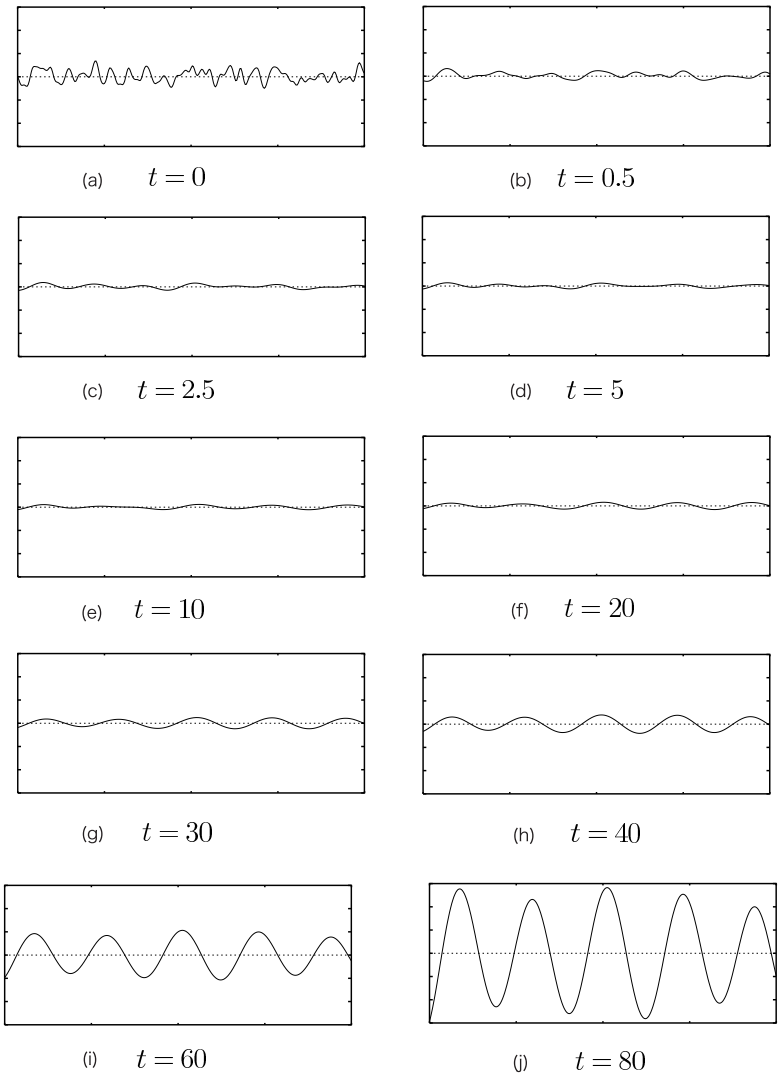

Fig. 5. Snapshots of spatial profiles of u component for numerical solutions of (2.18) around the uniform steady state in a small window $0 < x < 8\pi$, $-0.00015 < y < 0.00015$ under the values of parameters (2.21) when $d_2 = 1.20$; (a) $t = 0$, (b) $t = 0.5$, (c) $t = 2.5$, (d) $t = 5$, (e) $t = 10$, (f) $t = 20$, (g) $t = 30$, (h) $t = 40$, (i) $t = 60$, (j) $t = 80$. They show the dynamics of (2.18) in the early stage. The fully developed Turing patterns with the amplitude about 0.25 are out of this small window.

state is a *saddle point* in the PDE dynamics. In other words, the uniform steady state becomes unstable after super-critical bifurcation, however, it attracts almost every solution in the early stage of the PDE dynamics. Consequently, the uniform steady state plays crucial role to determine direction of time evolution of solutions. Therefore, the criterion that the maximizer of the dispersion relation predicts the wavenumber of the Turing pattern can be applicable if the uniform steady state attracts solutions starting from random initial disturbances to its sufficiently small neighborhood (see Fig. 6).

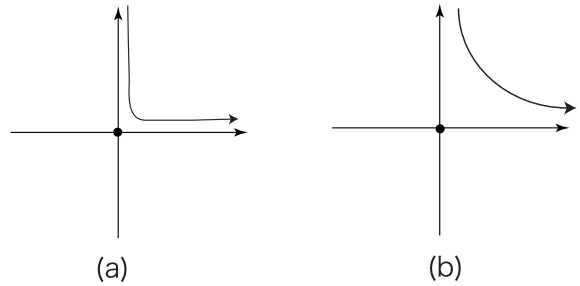

Fig. 6. A heuristic picture of the dynamics around the uniform steady state. In the case (a), solutions go through a sufficiently small neighborhood of the uniform steady state, so that the maximizer of the dispersion relation can predict the wavenumber to be selected. On the other hand, in case (b), solutions do not come close enough to the uniform steady state, so that the criterion may not be effective.

After an almost instantaneous smoothing process induced by diffusion effect at the initial stage, the solutions of (2.18) virtually become spatially constant. Therefore, the diffusion effect subsides and the subsequent PDE dynamics of (2.18) closely follows the ODE dynamics given by

$$\begin{cases} \tau_1 u_t = \alpha u - \sigma u^3 - \beta v, \\ \tau_2 v_t = \beta u - \gamma v, \end{cases} \tag{3.1}$$

in which $(\bar{u}, \bar{v}) = (0, 0)$ is a stable equilibrium. This means that the temporary attraction of random initial disturbances to the uniform steady state is characterized by the eigenvalues of the linearization of (3.1) at $(\bar{u}, \bar{v}) = (0, 0)$, i.e.,

$$\mu_1 = \frac{-(\gamma\tau_1 - \alpha\tau_2) + \sqrt{(\gamma\tau_1 + \alpha\tau_2)^2 - 4\tau_1\tau_2\beta^2}}{2\tau_1\tau_2},$$

$$\mu_2 = \frac{-(\gamma\tau_1 - \alpha\tau_2) - \sqrt{(\gamma\tau_1 + \alpha\tau_2)^2 - 4\tau_1\tau_2\beta^2}}{2\tau_1\tau_2}.$$

Notice that μ_j $(j = 1, 2)$ are not dependent on a bifurcation parameter d_2, and

$$\lambda_j(0; d_2) = \mu_j \quad (j = 1, 2),$$

where $\lambda_j = \lambda_j(s; d_2)$ $(j = 1, 2)$ are the dispersion relations given by (2.9). As for the example treated in the previous section, we find that

$$\operatorname{Re}\mu_1 \ll 0 < \max_s \lambda_1(s; d_2) \tag{3.2}$$

for $d_2 > d_2^c$. In fact, under the parameters (2.21),

$$\mu_1 = -0.5 \ll 0 < \max_s \lambda_1(s; d_2)$$

holds (for example, $0.05983 \approx \max_s \lambda_1(s; d_2)$ when $d_2 = 1.2$). We propose (3.2) as a practical condition to guarantee that the maximizer of the dispersion relation can predict the wavenumber of the Turing pattern generated from a small random initial disturbance.

In order to examine the validity of the above condition, we choose parameters so as to $\operatorname{Re}\mu_1 \lesssim 0$. After verifying (2.10)–(2.14), we numerically solve (2.18) under the same values of parameters as (2.21) except $\tau_2 = 1.99$, i.e.,

$$\begin{aligned} &d_1 = 0.25, \quad \alpha = 1.0, \quad \beta = 1.5, \quad \gamma = 2.0, \\ &\sigma = 1.0, \quad \tau_1 = 1.0, \quad \tau_2 = 1.99 \quad \text{and} \quad \varepsilon = 0.0001. \end{aligned} \tag{3.3}$$

For these parameters, the bifurcation diagram given by $d_2 = \hat{d}_2(s)$ is same as Fig. 1, however, the behavior of the critical dispersion relation around $s = 0$ is different from Fig. 2 as follows:

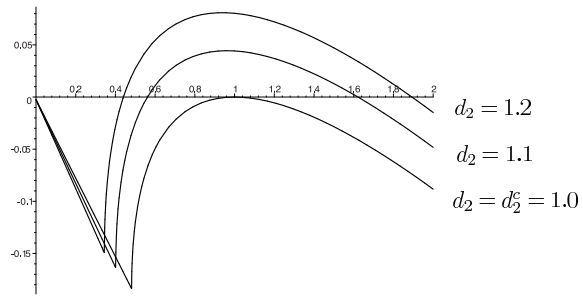

Fig. 7. The behavior of the critical dispersion relation $\lambda_1 = \lambda_1(s; d_2)$ for $d_2 = 1.0, 1.1, 1.2$ under (3.3). It is corresponding to the maximum of the real parts of the roots of $G(\lambda, s; d_2) = 0$, which has a double root at the singular point of the above curves.

It should be noted that the critical dispersion relation satisfies usual conditions for the Turing bifurcation as seen in [5, 10, 11] because (2.10)–(2.14) hold. In this case, $\mu_1 \approx -0.00251 + 0.3544i$ and $\mu_2 \approx -0.00251 - 0.3544i$, so that solutions starting from random initial disturbances oscillate and approach the uniform steady state in the early stage of the dynamics when $d_2 = 1.20$. In contrast to the previous case as seen in Fig. 5, the solutions do not come close enough to the uniform steady state (see Fig. 6 (b)).

In a similar manner to the previous section, under the values of parameters (3.3) with $d_2 = 1.20$, we numerically verify that the Turing patterns appear from the uniform steady state, and find that $k_s(1.20) \approx 1.00$ by the following statistical result.

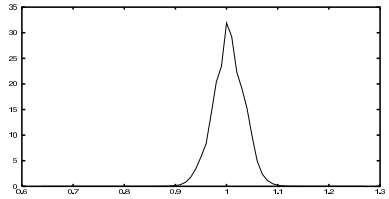

k	0.95	0.96	0.97	0.98	0.99	1.00
$\hat{u}(k)$	5.74	8.32	14.13	20.38	23.45	31.90

k	1.01	1.02	1.03	1.04	1.05	1.06
$\hat{u}(k)$	29.26	22.28	19.11	15.21	9.73	4.90

Fig. 8. The average of the Fourier power spectra of $u(x, T)$ for 30 random initial data.

Considering the accuracy of our numerical computation, the above result shows that the wavenumber of the Turing pattern deviates from the maximizer of the dispersion relation to the right because $k_u(1.20) \approx 0.97$ by virtue of (2.20). A reason for this deviation is due to that almost every solution starting from a random initial data can not come close enough to the uniform steady state since the condition (3.2) does not hold under (3.3).

Although the above result is based on a concrete example (2.1), it seems to be valid for general two component reaction-diffusion systems. In fact, after appropriate spatio-temporal rescaling, without loss of generality, we may suppose that general two component reaction-diffusion system

$$\begin{cases} \tau_1 u_t = d_1 u_{xx} + f(u, v), \\ \tau_2 v_t = d_2 v_{xx} + g(u, v) \end{cases} \tag{3.4}$$

satisfies

$$f_v(\bar{u}, \bar{v}) = -g_u(\bar{u}, \bar{v}), \tag{3.5}$$

where $(\bar{u}, \bar{v})$ denotes the uniform steady state. The minus sign of (3.5) means that two types of components with opposite interaction such as activator-inhibitor is necessary to produce the Turing patterns. Recalling our experimental fact that the nonlinearity of reaction-diffusion systems does not explicitly affect the wavenumber to be selected, we may consider that a mode selection mechanism for the Turing patterns of (3.4) is similar to the one of (2.1). Actually, in our numerical experiments, we could not find out a concrete example of two component reaction-diffusion system such that the wavenumber of the Turing pattern is not less than the maximizer of the dispersion relation.

Next, we give another example which indicates that the wavenumber of the Turing pattern deviates from the maximizer of the dispersion relation to the left. It is not so easy to find out such an example because we have to consider three or

more component reaction-diffusion systems with many parameters. Let us consider a three component system

$$\begin{cases} \tau_1 u_t = d_1 u_{xx} + \alpha u - \sigma u^3 - \beta v - \nu w, \\ \tau_2 v_t = d_2 v_{xx} - \gamma v + \beta u - c w, \\ \tau_3 w_t = d_3 w_{xx} - \rho w + \nu u + c v, \end{cases} \tag{3.6}$$

which consists of one activator u and two inhibitors v and w. When $c = 0$, (3.6) was studied in [1] which concerned with the dynamics of localized patterns such as a traveling spot. Moreover, (3.6) with $c = 0$ has a skew-gradient structure explained in the next section. The parameter c describes the internal interaction between two inhibitors.

We consider the Turing patterns on the trivial steady state $(\bar{u}, \bar{v}, \bar{w}) = (0, 0, 0)$, in which we choose d_2 as a bifurcation parameter. In order to seek suitable value of each parameter, we set $d_3 = 0$ and carry out a concrete calculation with the aid of computer algebra. Then we consider a situation for small $d_3 > 0$.

In the same fashion as the two-component system (2.1) treated in the previous section, when $d_3 = 0$, we have

$$d_2 = \hat{d}_2(s) = \frac{\beta^2}{s(\alpha - s d_1 - \nu^2/\rho)} - \frac{\gamma}{s} - \frac{c^2(\alpha - s d_1)}{\rho s(\alpha - s d_1 - \nu^2/\rho)}. \tag{3.7}$$

Differentiating (3.7) with respect to s, we find that the bifurcation point

$$s_c = k_c^2 = \frac{-h_1 + \sqrt{h_2}}{d_1 \rho(\gamma\rho + c^2)} \quad \text{and} \quad d_2^c = \hat{d}_2(s_c), \tag{3.8}$$

where

$$h_1 := \rho\{(\beta^2 - \alpha\gamma)\rho + \nu^2\gamma - c^2\alpha\} > 0 \tag{3.9}$$

and

$$h_2 := (\beta\rho + \nu c)(\beta\rho - \nu c)h_1 > 0. \tag{3.10}$$

In this case, we expect that the Turing pattens appear for $d_2 > \hat{d}_2(k^2)$ near the bifurcation point (k_c, d_2^c) under appropriate values of parameters.

Next, we consider the critical dispersion relation. In a similar manner to the previous section, we consider

$$G(\lambda, s; d_2) := \theta_1\theta_2\theta_3 + \beta^2\theta_3 + \nu^2\theta_2 + c^2\theta_1 = 0, \tag{3.11}$$

where $\theta_1 = \lambda\tau_1 + s d_1 - \alpha$, $\theta_2 = \lambda\tau_2 + s d_2 + \gamma$ and $\theta_3 = \lambda\tau_3 + s d_3 + \rho$. Notice that $G(\lambda, s; d_2)$ does not include σ which indicates the intensity of nonlinearity. Suppose that $G(\lambda, s; d_2) = 0$, a cubic equation in λ, gives dispersion relations

$$\lambda_j = \lambda_j(s; d_2) \quad (j = 1, 2, 3)$$

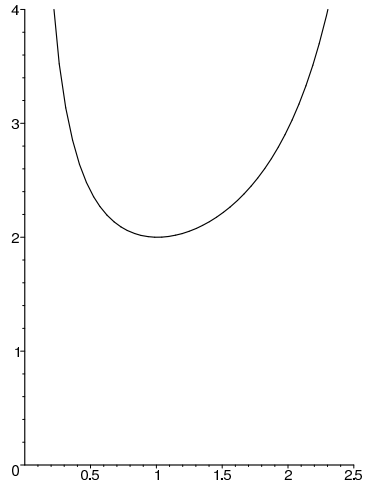

Fig. 9. The graph of $d_2 = \hat{d}_2(s)$ when $d_1 = 0.25$, $d_3 = 0.01$, $\alpha = c = \gamma = \rho = 1.0$, $\beta = 1.5$, $\nu = 0.5$. The Turing patterns appear for $d_2 > \hat{d}_2(s)$. This graph is obtained by a perturbation of (3.7).

satisfying the following properties:

$$\operatorname{Re}\lambda_1(s; d_2) < 0 \text{ for all } s \text{ and } d_2 < d_2^c, \tag{3.12}$$

$$\lambda_1(s_c; d_2^c) = 0 \text{ and } \operatorname{Re}\lambda_1(s; d_2^c) < 0 \text{ for } s \neq s_c, \tag{3.13}$$

$$\lambda_1(s; d_2) \text{ is real valued near the bifurcation point } (s_c, d_2^c), \tag{3.14}$$

$$\frac{\partial}{\partial d_2}\lambda_1(s; d_2)\bigg|_{(s,d_2)=(s_c,d_2^c)} > 0, \tag{3.15}$$

$$\operatorname{Re}\lambda_2(s; d_2), \operatorname{Re}\lambda_3(s; d_2) < 0 \text{ for all } s \text{ and } d_2. \tag{3.16}$$

When $d_3 = 0$, we choose the following values of parameters

$$\begin{aligned} &d_1 = 0.25, \quad \alpha = c = \gamma = \rho = 1, \quad \beta = 1.5, \quad \nu = 0.5, \\ &\tau_1 = \tau_2 = \tau_3 = 1 \end{aligned} \tag{3.17}$$

so as to satisfy (3.12)–(3.16). For these parameters, we find $s_c = k_c^2 = 1.0$ and $d_2^c = 2.0$ by virtue of (3.8).

We now take a small $d_3 > 0$, say $d_3 = 0.01$. In this case, we can numerically obtain the graph of $d_2 = \hat{d}_2(s)$, and verify

$$(k_c, d_2^c) = (1.003754156, 1.999944522) \approx (1.00, 2.00),$$

and the conditions (3.12)–(3.16). Moreover, Fig. 10 (a) shows the behavior of $\lambda_1 = \lambda_1(s; d_2)$ when $d_3 = 0.01$ and (3.17).

When $d_3 = 0.01$, $\sigma = 1.0$ and (3.17), we numerically solve (3.6) for $d_2 = 2.05$, 2.10 and 2.20 corresponding to $|d_2 - d_2^c|/d_2^c \approx 0.025$, 0.05 and 0.1, respectively. By

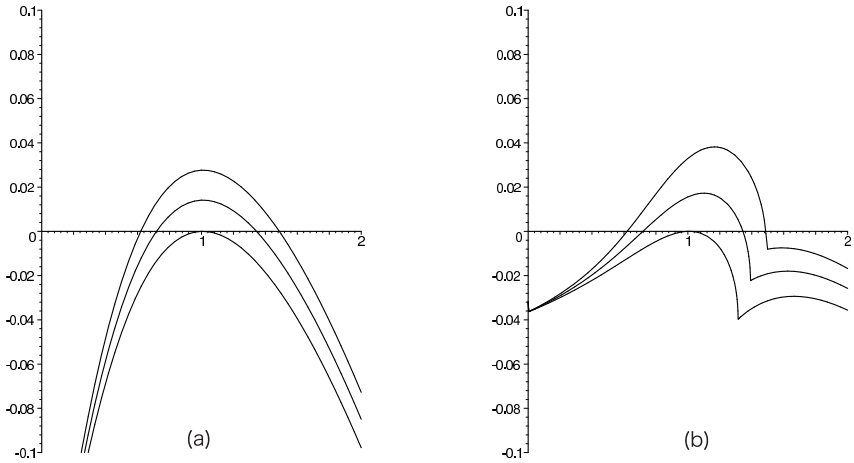

Fig. 10. The behavior of the critical dispersion relation $\lambda_1 = \lambda_1(s; d_2)$ for $d_2 = 2.0, 2.1, 2.2$ when $d_1 = 0.25$, $d_3 = 0.01$, $\alpha = c = \gamma = \rho = 1.0$, $\beta = 1.5$, $\nu = 0.5$, $\tau_1 = \tau_2 = 1.0$. It is corresponding to the maximum of the real parts of three roots of $G(\lambda, s; d_2) = 0$. (a) $\tau_3 = 1.0$, (b) $\tau_3 = 10.0$. $G(\lambda, s; d_2) = 0$ has a double real root at the singular point of curves in (b).

using the pseudo-spectral method and the discrete FFT as applied to (2.18), we can solve

$$\begin{cases} \tau_1 u_t = d_1 u_{xx} + \alpha u - \sigma u^3 - \beta v - \nu w, \\ \tau_2 v_t = d_2 v_{xx} - \gamma v + \beta u - c w, \\ \tau_3 w_t = d_3 w_{xx} - \rho w + \nu u + c v, \\ u(x,0) = \varepsilon u_0(x), \quad v(x,0) = \varepsilon v_0(x), \quad w(x,0) = \varepsilon w_0(x), \\ 0 < x < L, \quad 0 < t < T, \end{cases} \tag{3.18}$$

where $L = 200\pi$, $\varepsilon = 0.0001$ and $u_0(x), v_0(x), w_0(x) \in (-1/2, 1/2)$ are uniform distributions generated by pseudo-random numbers. For sufficiently large T, the spatial profile of $u(x, T)$ looks like a sinusoidal function with a particular wave-number. Computing the power spectra of $u(x, T)$ for 30 random initial data, and taking their average, we obtain the following results:

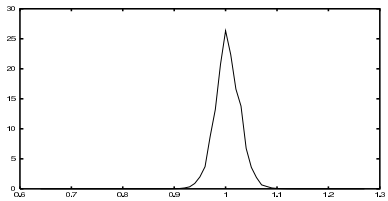

k	0.95	0.96	0.97	0.98	0.99	1.00
$\hat{u}(k)$	1.99	3.69	8.72	13.22	20.71	26.34

k	1.01	1.02	1.03	1.04	1.05	1.06
$\hat{u}(k)$	22.35	16.62	13.78	6.74	3.58	1.90

Fig. 11. The average of the Fourier power spectra of $u(x, T)$ for 30 random initial data when $d_2 = 2.2$.

Table 2. The selected wavenumber $k_s(d_2)$ for $d_2 = 2.05$, 2.10 and 2.20.

d_2	2.05	2.10	2.20
$k_u(d_2)$	1.00	1.00	1.00
$k_s(d_2)$	1.00	1.00	1.00

The above table shows $k_s(d_2) \approx k_u(d_2)$, where $k_u(d_2)$ is given by the maximizer of the critical dispersion relation $\lambda_1 = \lambda_1(s; d_2)$. This result supports that the maximizer of the dispersion relation can predict the wavenumber of the Turing pattern generated from a small random initial disturbance under the condition (3.2). In fact, μ_1 is real and

$$\mu_1 \approx -0.21445 \ll 0 < \max_s \lambda_1(s; d_2)$$

holds (for example, $0.02765 \approx \max_s \lambda_1(s; d_2)$ when $d_2 = 2.2$), so that (3.2) holds.

On the other hand, we numerically solve (3.18) under the same values of parameters as (3.17) except $\tau_3 = 10$, i.e.,

$$\begin{aligned} &d_1 = 0.25, \quad d_3 = 0.01, \quad \alpha = c = \gamma = \rho = 1, \quad \beta = 1.5, \quad \nu = 0.5, \\ &\tau_1 = \tau_2 = 1, \quad \tau_3 = 10. \end{aligned} \tag{3.19}$$

In this case, we can numerically verify (3.12)–(3.16) and the behavior of the critical dispersion relation as in Fig. 10 (b). In the same way as the previous case, we solve (3.18) under (3.19) and obtain the following statistical results:

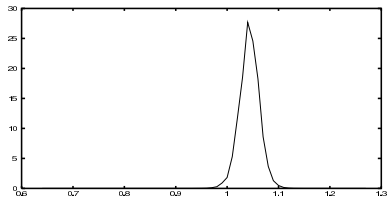

k	0.99	1.00	1.01	1.02	1.03	1.04
$\hat{u}(k)$	0.90	1.81	5.29	11.76	18.50	27.68

k	1.05	1.06	1.07	1.08	1.09	1.10
$\hat{u}(k)$	24.57	18.26	8.60	3.67	1.28	0.48

Fig. 12. The average of the Fourier power spectra of $u(x, T)$ for 30 random initial data when $d_2 = 2.2$.

Table 3. The selected wavenumber $k_s(d_2)$ for $d_2 = 2.05$, 2.10 and 2.20.

d_2	2.05	2.10	2.20
$k_u(d_2)$	1.03	1.05	1.08
$k_s(d_2)$	1.02	1.03	1.04

Considering the accuracy of our numerical computations, we find that $k_s(d_2)$ deviates from $k_u(d_2)$ to the left. In this case, μ_1 is a complex number with the non-zero imaginary part, and

$$\operatorname{Re}\mu_1 \approx -0.03178 < 0 < \max_s \lambda_1(s; d_2)$$

holds (for example, $0.03814 \approx \max_s \lambda_1(s; d_2)$ when $d_2 = 2.2$), so that (3.2) does not hold.

In addition, we verify that the selected wavenumber $k_s(d_2)$ do not depend on σ the coefficient of the nonlinear term because the almost same numerical results as Tables 2 and 3 are obtained for $\sigma = 0.1$ and $\sigma = 10$. This implies that our numerical experiments are done in a small neighborhood of the bifurcation point.

Thus, it is possible for three component reaction-diffusion systems that the wavenumber of the Turing pattern deviates from the maximizer of the dispersion relation to the left.

Remark 2. The Routh–Hurwitz theorem [10, Appendix 2] is an useful tool for checking the conditions (3.12)–(3.16) which impose strict restrictions on a range of parameters. In general reaction-diffusion systems with three or more components, however, it is not easy to verify (3.12)–(3.16) because $G(\lambda, s; d_2) = 0$ becomes a quite involved and lengthy equation.

Remark 3. When $c = 0$, we can not take τ_3 relatively larger than τ_1 and τ_2 satisfying (3.12)–(3.16), so that the deviation from the predicted wavenumber to the left can not be observed. We can not give a rigorous proof of this fact, however, we may expect that the parameter c plays a crucial role in our numerical experiments.

4. Discussion

As we have observed in the arguments so far, our mode selection problem for the Turing patterns is a statistical problem. We have examined the dynamics around the uniform steady state near the bifurcation point, and propose a practical condition to guarantee the criterion that the wavenumber of the Turing pattern generated from a small random initial disturbance can be predicted by the maximizer of the dispersion relation.

In this section, we briefly mention some relevant subjects and further problems related to the results presented in previous sections. They suggest us to reconfirm the validity of well accepted assertions concerning pattern selection from both experimental and theoretical points of view.

4.1. Mode selection for gradient/skew-gradient systems

One of useful approach to study pattern selection problem is to find a free energy (variational principle), which determines direction of time evolution of systems. In other words, the selected pattern can be indicated by the (global) minimizer of free energy. This is intuitively natural, however, is not always true. In fact, the minimizer of a free energy does not always have the largest basin of attraction. As for a mode selection problem for the Turing patterns generated from small random initial disturbances, the dispersion relation plays a more important role than a free energy. In order to understand this fact, we recall reaction-diffusion systems with *gradient/skew-gradient structure* [7, 14].

A reaction-diffusion system

$$T\mathbf{u}_t = D\Delta\mathbf{u} + Q\nabla_u F(\mathbf{u}), \quad \mathbf{u} = (u_1, \dots, u_n)^{\mathrm{T}} \tag{4.1}$$

is said to have gradient/skew-gradient structure when (4.1) satisfies the following assumptions:

(A1) T is a non-degenerate positive diagonal matrix.

(A2) D is a regular matrix satisfying $D^{\mathrm{T}}Q = QD$, where Q is a symmetric matrix with $Q^2 = I_n$.

(A3) $f(\mathbf{u}) = Q\nabla_u F(\mathbf{u})$, where $F = F(\mathbf{u})\colon \mathbf{R}^n \to \mathbf{R}$ is a smooth function.

Under the above assumptions, we immediately see that (4.1) has a (skew) free energy defined by

$$\mathcal{E}[\mathbf{u}] = \int \left\{ \frac{1}{2}\langle\!\langle D\nabla\mathbf{u}, Q\nabla\mathbf{u}\rangle\!\rangle - H(\mathbf{u}) \right\} dx,$$

where

$$\langle\!\langle D\nabla\mathbf{u}, Q\nabla\mathbf{u}\rangle\!\rangle := \sum_{i,j} d_{ij}\nabla u_j \cdot q_{ij}\nabla u_j.$$

In fact, we can easily (formally) check that the (skew) energy equation

$$\frac{d}{dt}\mathcal{E}[\mathbf{u}(x,t)] = -\int \langle \mathbf{u}_t, QT\mathbf{u}_t\rangle \, dx$$

holds, where $\langle\,\cdot\,,\,\cdot\,\rangle$ denotes the usual inner product defined on $\mathbf{R}^n$. (4.1) is said to have gradient structure when QT is nonnegative symmetric, and skew-gradient structure otherwise. As for (2.1), we can easily see that

$$\frac{d}{dt}\mathcal{E}[u(x,t), v(x,t)] = -\int (\tau_1 u_t^2 - \tau_2 v_t^2)\, dx$$

holds, where $\mathcal{E}[u,v]$ is given by

$$\mathcal{E}[u,v] = \int \frac{d_1}{2}u_x^2 - \frac{d_2}{2}v_x^2 - F(u,v)\, dx$$

and $F(u,v) = \alpha u^2/2 - u^4/4 - \beta uv + \gamma v^2/2$. Therefore, (2.1) has a skew-gradient structure for $\tau_2 > 0$ while gradient structure for $\tau_2 = 0$. In both cases, the selected wavenumber is given by the maximizer of the critical dispersion relation under a condition such as (3.2). Notice that it is different from the minimizer of a (skew) free energy. In other words, the gradient system (2.1) with $\tau_2 = 0$ is a typical example such that the pattern to be selected is not corresponding to the minimizer of a free energy. As was mentioned in [7], however, we may expect that the selected wavenumber is not greater than the minimizer of a (skew) free energy under a certain condition as (3.2).

4.2. Scalar equation vs. system

It is well known [9] that one-dimensional scalar reaction-diffusion equation can not exhibit the Turing patterns. However, a fourth order scalar equation such as the Swift–Hohenberg equation has a family of spatially periodic bifurcating stationary solutions which are considered as the Turing patterns. In fact, as was mentioned in [8], such fourth order scalar equation can be formally rewritten as two component reaction-diffusion system. For example, the Swift–Hohenberg equation

$$u_t = \alpha u - (1 + \partial_{xx})^2 u - u^3 \tag{4.2}$$

can be rewritten as a 2-component gradient system (4.1) by setting $(u_1, u_2) = (u, v)$, where $v = u + u_{xx}$ and

$$T = \begin{pmatrix} 1 & 0 \\ 0 & 0 \end{pmatrix}, \quad D = \begin{pmatrix} 0 & -1 \\ 1 & 0 \end{pmatrix}, \quad Q = \begin{pmatrix} 1 & 0 \\ 0 & -1 \end{pmatrix},$$

$$F = F(u, v) = \frac{\alpha}{2}u^2 - \frac{1}{4}u^4 - uv + \frac{1}{2}v^2.$$

We immediately find that the dispersion relation for (4.2) is given by

$$\lambda_1 = \alpha - (1 - k^2)^2, \tag{4.3}$$

which implies that bifurcating stationary solutions with wavenumber $k \approx 1$ appear for $\alpha > 0$. Notice that the dispersion relation of a scalar equation has a single branch. Substituting $u = \varepsilon \cos(kx)$ to (4.2) and using the long wavelength approximation $\cos^3(kx) = (3\cos(kx) + \cos(3kx))/4 \approx 3\cos(kx)/4$, we can easily obtain

$$u = \varepsilon \cos(kx) + O(\varepsilon^3), \quad \varepsilon = 2\sqrt{(\alpha - (1 - k^2)^2)/3}, \tag{4.4}$$

which gives a family of bifurcating stationary solutions of (4.2) for $\alpha > 0$. In a similar manner to the previous sections, we investigate a mode selection problem for spatially periodic patterns (4.4) near the bifurcation point. In the scalar equation (4.2), for any small random initial disturbance, the Fourier power spectrum of $u(x, T)$ for sufficiently large $T > 0$ has a clear bell shape independent of initial data as in Fig. 13. In this case, the deviation from the predicted wavenumber by the dispersion relation can not be observed. Therefore, the resulting pattern seems to be selected in a deterministic way, and it is the most outstanding difference between fourth order scalar equations such as (4.2) and reaction-diffusion systems such as (2.1). This fact is characteristic of a scalar equation, and may be one of reason why a scalar equation is mainly used for verifying the validity of various assertions concerning pattern selection [2, 12]. In the above scalar equation, the dispersion relation (4.3) satisfies the condition (3.2). For a scalar equation, it may be a necessary condition that the wavenumber of a bifurcating pattern seems to be selected in a deterministic way.

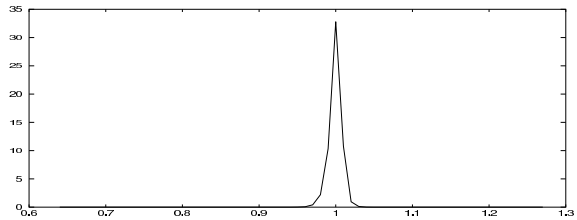

Fig. 13. The Fourier power spectrum of $u(x,T)$ for solutions of (4.2) for $T = 2000$ when $\alpha = 0.01$.

4.3. Propagation of the Turing patterns

We have investigated a mode selection problem for the Turing patterns generated from small initial disturbances. We are also interested in a mode selection problem for spatially periodic patterns generated from sufficiently localized initial data. In this case, a small localized initial perturbation evolves into the fully developed Turing pattern on a sufficiently small region, then spreading into the uniform steady state as in Fig. 14, and eventually covering the entire region.

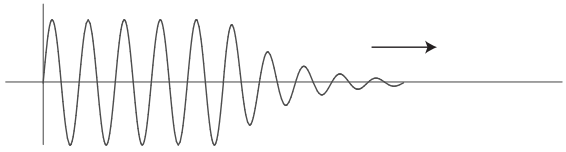

Fig. 14. A schematic picture of the Turing pattern spreading into the uniform steady state.

Our problem is to predict the speed of a pattern forming front and the wavenumber of a spatially periodic stationary pattern far behind the front. For such problems, we may suppose that the speed of a front is determined by the dynamics of the leading edge of the front, which can be analyzed by the linearization of the dynamics around the uniform steady state. According to [11, 12], we briefly review a standard procedure to predict the speed of a pattern forming front by using the dispersion relation, and consider the wavenumber of the Turing pattern far behind the front.

Let ψ be a perturbation of the form $\psi \sim e^{-i\omega t+ikx}$. In the same way as the argument in Section 2, substituting $\psi \sim e^{-i\omega t+ikx}$ into the linearization of a given equation around the uniform steady state, we obtain the dispersion relation, expressing as a function of k,

$$\omega = \omega(k).$$

Here, ω and k are allowed to be complex numbers. That is, $k^i := \operatorname{Im} k$ determines the order of spatial decay at infinity and the shape of the envelop, while $k^r := \operatorname{Re} k$ indicates the wavenumber within the envelop. Moreover, $\omega^i := \operatorname{Im} \omega$ determines whether the perturbation decays or grows, and $\omega^r := \operatorname{Re} \omega$ describes whether the temporal behavior is oscillatory or monotone.

For each fixed k_i, we assume that the temporal growth rate ω_i, as a function of the wavenumber k_r, has the functional form as in Fig. 15. Under the above assumption, we consider the fastest growing wavenumber defined by

$$\frac{\partial \omega_i}{\partial k_r} = 0, \quad \frac{\partial^2 \omega_i}{\partial k_r^2} < 0$$

for each fixed k_i, which determines k_r as a function of k_i. Then we introduce the envelop velocity

$$c = c(k_i) = \frac{\omega_i}{k_i},$$

and seek the minimizer of $c = c(k_i)$ defined by

$$\frac{\partial c}{\partial k_i} = \frac{1}{k_i^2}\left(\frac{\partial \omega_i}{\partial k_i} k_i - \omega_i\right) = 0.$$

Thus we obtain the *linear marginal stability criterion*

$$c^* = \frac{\omega_i}{k_i} = \frac{\partial \omega_i}{\partial k_i}, \quad \frac{\partial \omega_i}{\partial k_r} = 0, \tag{4.5}$$

which gives the selected wave speed c^* and the corresponding wavenumber k_r^* at the leading edge of a front. We may expect that this criterion is valid near the bifurcation point, where nonlinearity is not significant.

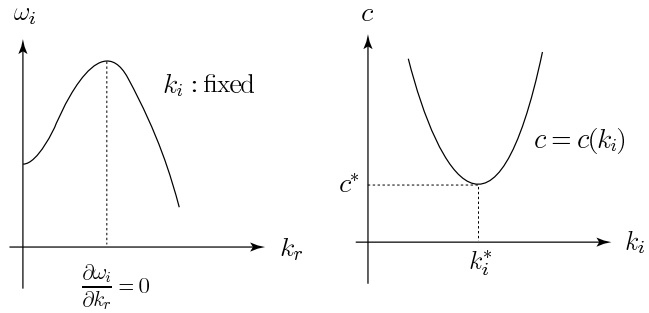

Fig. 15. The functional form of $\omega_i = \omega_i(k_r)$ for fixed k_i, and $c = c(k_i)$.

Next, we consider the wavenumber of a spatially periodic stationary pattern far behind a pattern forming front, which is different from k_r^*. In the moving frame with the speed c^*, the temporal profile of a solution in the leading edge is oscillatory, which is described by $e^{-i(\omega_r^* - k_r^* c^*)t}$. Therefore, the nodes created at the leading edge pass any fixed position near the leading edge with the angular frequency $|\omega_r^* - k_r^* c^*|$. On the other hand, in this moving frame, the Turing pattern with the wavenumber q^* far behind a front has the wave speed c^*, so that the nodes pass a fixed position far behind the front with the angular frequency $c^* q^*$ in

the moving frame. Applying the *node conservation condition* $c^*q^* = |\omega_r^* - k_r^* c^*|$, we obtain

$$q^* = |\omega_r^*/c^* - k_r^*|. \tag{4.6}$$

For example, applying (4.5) and (4.6) to the Swift–Hohenberg equation (4.2), we have

$$c^* = \frac{4}{3\sqrt{3}}(2 + \sqrt{1+6\alpha})(-1 + \sqrt{1+6\alpha})^{1/2}, \tag{4.7}$$

$$q^* = \frac{3(3 + \sqrt{1+6\alpha})^{3/2}}{8(2 + \sqrt{1+6\alpha})}. \tag{4.8}$$

As reported in [3, 12], we can numerically confirm the validity of (4.8).

Thus we see that the linear marginal stability criterion and the node conservation condition can predict the speed of a pattern forming front and the wavenumber of the Turing pattern far behind the front for a scalar equation as (4.2). However, noting the difference between scalar equations and systems as mentioned before, and recalling our results concerning the wavenumber of the Turing patterns generated from random initial disturbances, we should examine whether or not c^* and q^* exactly correspond to the speed of a front and the wavenumber of the Turing pattern far behind the front for reaction-diffusion systems. Our investigation is now in progress, and will be reported in a separate paper.

5. Summary

In this paper, we investigate a mode selection problem for the Turing patterns generated from small initial disturbances in one-dimensional reaction-diffusion systems on a sufficiently large domain. We examine the validity of a widely accepted criterion that the wavenumber of the Turing pattern exactly corresponds to the maximizer of the dispersion relation. This criterion asserts that the wavenumber of the Turing pattern observed with the highest probability is given by the maximizer of the dispersion relation.

For our problem, it is a simple but important fact that the uniform steady state is a saddle point in the PDE dynamics defined by reaction-diffusion systems. That is, the uniform steady state becomes unstable after super-critical bifurcation, however, it attracts almost every solution in the early stage of the PDE dynamics. The dominant part of the dynamics of this stage can be expressed by the ODE derived from the PDE without diffusion terms. This implies that the attractivity of solutions for the PDE starting from random initial disturbances to the uniform steady state is characterized by the eigenvalues of the linearized ODE. Therefore, in many practical applications, it is to be checked a condition that all the eigenvalues of the linearized ODE at the uniform steady state are far away from the real axis to the left. In fact, the criterion is not always true if the condition is not satisfied.

As for pattern selection problems, useful and practical selection criteria have been proposed, however, they are not fully understood from a mathematical view-

point. Therefore, the accumulation of basic knowledge as presented in this paper is indispensable for precise understanding of such criteria in various problems for pattern selection which is one of fundamental topics of pattern formation theory.

Acknowledgment. The author expresses his sincere gratitude to Professors Masayasu Mimura, Toshiyuki Ogawa and Kunimochi Sakamoto for their helpful comments and advices to complete this work. This work was supported in part by Grant-in-Aid for Scientific Research (C) No. 18540120, JSPS, Japan.

References

[1] M. Bode, A.W. Liehr, C.P. Schenk and H.-G. Purwins, Interaction of dissipative solitons: particle-like behavior of localized structures in a three-component reaction-diffusion system. Physica D, **161** (2002), 45–66.
[2] M.C. Cross and P.C. Hohenberg, Pattern formation outside of equilibrium. Rev. Mod. Phys., **65** (1993), 851–1112.
[3] G. Dee and J.S. Langer, Propagating pattern selection. Phys. Rev. Lett., **50** (1983), 383.
[4] J.C. Eilbeck, The pseudo-spectral method and following in reaction-diffusion bifurcation studies. SIAM J. Sci. Stat. Comput., **17** (1986), 599–610.
[5] G. Iooss and D.D. Joseph, Elementary Stability and Bifurcation Theory. Springer-Verlag, 1980.
[6] Y. Kuramoto, Chemical Oscillations, Waves and Turbulence. Springer-Verlag, 1984.
[7] M. Kuwamura, On the Turing patterns in one-dimensional gradient/skew-gradient dissipative systems. SIAM J. Appl. Math., **65** (2005), 618–643.
[8] M. Kuwamura and E. Yanagida, Krein's formula for indefinite multipliers in linear periodic Hamiltonian systems. J. Differential Equations, **230** (2006), 446–464.
[9] H. Matano, Asymptotic behavior and stability of solutions of semilinear diffusion equations. Publ. Res. Inst. Math. Sci., **15** (1979), 401–485.
[10] J.D. Murray, Mathematical Biology, 2nd edition. Springer-Verlag, 1993.
[11] Y. Nishiura, Far-from-Equilibrium Dynamics. Transl. Math. Monogr., **209**, AMS, Providence, RI, 2002.
[12] W. van Saarloos, Front propagation into unstable states. Physics Reports, **386** (2003), 29–222.
[13] A.M. Turing, The chemical basis of morphogenesis. Phil. Roy. Soc. B, **237** (1952), 37–72.
[14] E. Yanagida, Standing pulse solutions in reaction-diffusion systems with skew-gradient structure. J. Dynamics Differential Equations, **4** (2000), 89–205.